Braided-Shape Electromagnetic Sensor for Screening Multiple Eggs Using 7-Tesla Magnetic Resonance Imaging

Daniel Hernandez, Yonghwa Jeong, and Kyoung-Nam Kim

***Abstract*— Magnetic resonance imaging (MRI)-based in-ovo studies have great potential for use in both the food industry and preclinical research, but there are still limitations in terms of simultaneously screening large numbers of eggs. This study proposes a novel electromagnetic (EM) sensor for the simultaneous acquisition of images of multiple eggs using MRI. The coil has a braid-like shape, in which the eggs are placed in the space between the turns. The proposed sensor can be extended to multiple braids while exhibiting similar performance in terms of magnetic field $|B_1|$ and signal-to-noise ratio (SNR). This work consists of design and validation with EM simulations, followed by a bench test and image acquisition. The images of multiple eggs are compared with a reference volume eight-channel loop coil array and single-loop coils. It was observed that the proposed coil can produce a uniform magnetic field $|B_1|$ for each egg, and a good SNR was acquired with MRI. The proposed coil offers an advantage by reducing the number of transmit/receive channels needed to image multiple eggs while maintaining the same image quality for each egg.**

***Index Terms*— Antennas, electromagnetic (EM) propagation in absorbing media, magnetic resonance imaging (MRI), near-field radiation pattern.**

I. Introduction

MAGNETIC resonance imaging (MRI) is an imaging modality that acquires anatomical and functional images of biological tissues [1]. MRI with ultrahigh-field strength such as 7-Tesla (7T) can generate images of high quality and resolution [2], [3]. In MRI, the image quality depends on the transmitted and received magnetic field, known as the $|B_1|$-field, which is generated by near-field antennas or coils. Although MRI is most commonly used for the imaging of humans and small animals, few studies have been performed to acquire the images of avian eggs [4]. They have focused on understanding the development and growth process of embryo structure. In particular, the fertilization of eggs can be analyzed using MRI without breaking the eggshell [5]. A similar analysis was performed using computed tomography [6] and acoustic resonant analysis [7]. The use of MRI has also been reported for in-ovo [8]. Studies based on eggs and embryos consider multiple samples for examination. For example, in [6], hundred eggs were tested, with computer tomography imaging modality. The images of eggs are then scanned at different time intervals such as daily scans during the period of embryo development until hatching.

The application of MRI in the poultry industry plays a vital role in optimizing the egg production process and ensuring product quality. By utilizing MRI technology, producers can make informed decisions about the quality of eggs through the analysis of acquired images. A recent development in the poultry industry involves the use of MRI to identify fertilized eggs, with the potential to scan approximately 9000 eggs per hour [9]. This advancement offers a promising tool for enhancing efficiency and accuracy in egg production and quality control processes.

In addition to the benefits of MRI in the imaging of eggs, a few caveats or limitations such as long scan time exist. Therefore, images for multiple eggs should be generated simultaneously to reduce the overall scan time. A common practice is to place the eggs inside a volume coil, such as a birdcage or loop array, in a cylindrical setup [10]. These coils are ideal for anatomical imaging of humans and small animals due to their dimensions. However, for multiple eggs, a $|B_1|$-field difference is generated between each egg since the $|B_1|$-field is spatial-dependent. Thus, images with different intensities are acquired, which could compromise the comparison between eggs. The number of eggs that can be placed in a volume coil is also limited by the relationship between the dimension of the coil and the performance of the $|B_1|$-field, especially at high frequencies such as 300 MHz for 7T scanners. In other words, a larger coil could accommodate more eggs; however, it results in field nonuniformity due to which images with different intensities and qualities are generated for each egg.

One possible solution to provide a uniform $|B_1|$-field for each egg would be to design individual coils for each egg

Manuscript received 13 February 2023; revised 25 August 2023; accepted 18 September 2023. Date of publication 3 October 2023; date of current version 20 December 2023. This work was supported by the Institute for Information and Communications Technology Promotion (IITP) Grant funded by the Korean Government [Ministry of Science, ICT and Future Planning (MSIP)] (Development of Precision Analysis and Imaging Technology for Biological Radio Waves) under Grant 2021-0-00490. *(Corresponding author: Kyoung-Nam Kim.)*

Daniel Hernandez is with the Neuroscience Research Institute, Gachon University, Incheon 21988, South Korea (e-mail: theasdwmove@gmail.com).

Yonghwa Jeong is with the Department of Health Sciences and Technology, GAIHST, Gachon University, Incheon 21999, South Korea (e-mail: ahron703@naver.com).

Kyoung-Nam Kim is with the Department of Biomedical Engineering, Gachon University, Seongnam 13120, South Korea (e-mail: kyoungnam.kim@gachon.ac.kr).

Color versions of one or more figures in this article are available at https://doi.org/10.1109/TAP.2023.3319690.

Digital Object Identifier 10.1109/TAP.2023.3319690

such as loop coils. The concept of multiple objects using multiple coils has been proposed for small animals [11], [12], [13]. The use of multiple coils for individual objects could simultaneously improve the scan time and maintain image quality. However, this concept works efficiently when the number of imaging objects is less than the number of available transmission and reception (TRx) channels in the scanner. As presented in a previous study, the number of tested eggs was approximately 100, which is greater than the number of available reception channels in a typical MRI scanner. To solve this problem, we have proposed the design of a coil capable of generating a uniform $|B_1|$-field for multiple eggs while using a single channel.

The coil is designed in the shape of a braid, in which the distance between the conductor lines resembles a circular loop coil. To validate our design, electromagnetic (EM) simulations were performed to test the performance of $|B_1|$-field. Based on the simulation results, we have built coils and performed bench tests to analyze the tuning and matching conditions. The design was tested by acquiring MR images of multiple eggs and was compared with a volume eight-channel array coil and multiple single-loop coils. It was observed that the proposed design is capable of producing a uniform magnetic $|B_1|$-field and good image quality for each egg.

The efficiency of the proposed coil plays a crucial role in revolutionizing the imaging process by enabling the acquisition of high-quality images of multiple eggs while utilizing fewer TRx channels. This efficiency translates to the ability to accommodate and image multiple eggs within a given volume space. By maximizing the coil's performance and optimizing its design, the proposed coil can effectively utilize the available space to acquire images of each individual egg. This not only enhances the imaging process, but also enables more efficient use of resources, making it possible to image a larger number of eggs within a confined space without compromising image quality.

II. Materials and Methods

A. Design

The proposed coil is designed in the shape of a braid that can be extended to multiple turns, as shown in Fig. 1(a). It consists of two layers, namely, upper (displayed in orange) and lower (displayed in blue) separated by a small distance in the vertical direction. The conductor lines follow the geometry of a half circumference, and the other half is extended such that it follows a continuous semicircular wave pattern. A similar geometry is used for the lower layers. From the top view, the coil looks like multiple loop coils; however, the difference is that for each turn, the upper and lower layers are not directly connected. A capacitor is placed at the intersection of the other half of the circumference of the next turn. Tuning capacitors are placed in both the upper and lower layers, as shown in Fig. 1(b). In the last turns, the capacitor is used to connect the upper and lower layers [Fig. 1(c)]. For symmetrical $|B_1|$-field performance, the source is placed on the center of the coil, as indicated in Fig. 1(a).

The design concept is based on the artificial creation of a loop coil at each turn. If the coil in Fig. 1(a) can be segmented

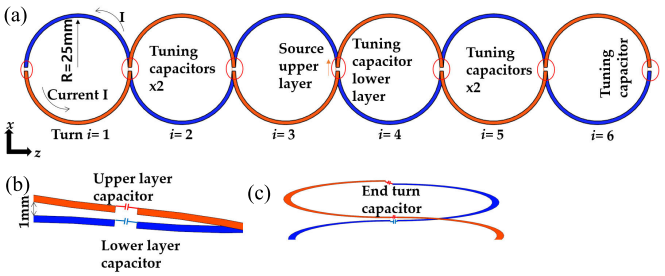

Fig. 1. Geometry of the: (a) braided coil for multiple eggs; (b) zoomed-in version of the upper and lower layers shows the position of the capacitors; and (c) capacitor at the end of the coil.

in the upper part (highlighted in orange), it would be the same as the semicircular segment of a loop coil, in which the current density will flow in the direction of the input source. For the second segment of the semicircle, the lower layer (blue) has the same direction as the current, thus creating an effect similar to that of the closed-loop coil. This can be understood better from the last turn of the coil, where the upper and lower layers are connected by a capacitor, thus allowing the continuous flow of current.

The proposed coil is represented using the Biot–Savart equation for a loop coil and extended to the proposed design. The mathematical representation of the upper layer for the coil laying on the xz plane can be described by extending the parametric equation of a circle, in which the parameter t varies only from 0 to π, which is similar to that of a semicircle. The proposed coil is composed of n number of turns along the z-axis; therefore, the x and z parametrization of the coil of n turns for segment i would be described as follows:

$$dxi = Rcos(t) + R + 2Ri, i = 0, 1, \ldots, n \quad (1.1)$$

$$dzi = Rsin(t)cons(2\pi i), i = 0, 1, \ldots, n \quad (1.2)$$

where R is the radius of the coil. Similarly, the bottom layer, which has the opposite direction of z value, can be represented as follows:

$$dxi = Rcos(t) + R + 2Ri, i = 0, 1, \ldots, n; t = 0 : \pi \quad (2.1)$$

$$dzi = -Rsin(t)cos(2\pi i), i = 0, 1, \ldots, n; t = 0 : \pi. \quad (2.2)$$

The Biot–Savart equation can be applied for the i-turn as a combination of (1.1) and (2.2) or (1.2) and (2.1) as follows:

$$Bi = \frac{\mu_0}{2\pi}\int_0^{\pi} \frac{\cos\theta dl}{y^2 + (R(4i\cos t + 4i^2{+}1))^2} + \int_{\pi}^{2\pi} \frac{\cos\theta dl}{y^2 + (R(4i\cos t + 4i^2{+}1))^2} \quad (3)$$

where the limits of integration are from 0 to π according to the semicircle. The magnetic field at the center of each turn for a distance y away from the plane of the coil is

$$B = \frac{\mu_0}{2\pi} \frac{1}{\left(y^2 + (R(4i\cos t + 4i^2 + 1))^2\right)^{3/2}}. \quad (4)$$

Equation (4) has the same value as the loop coil when i is zero.

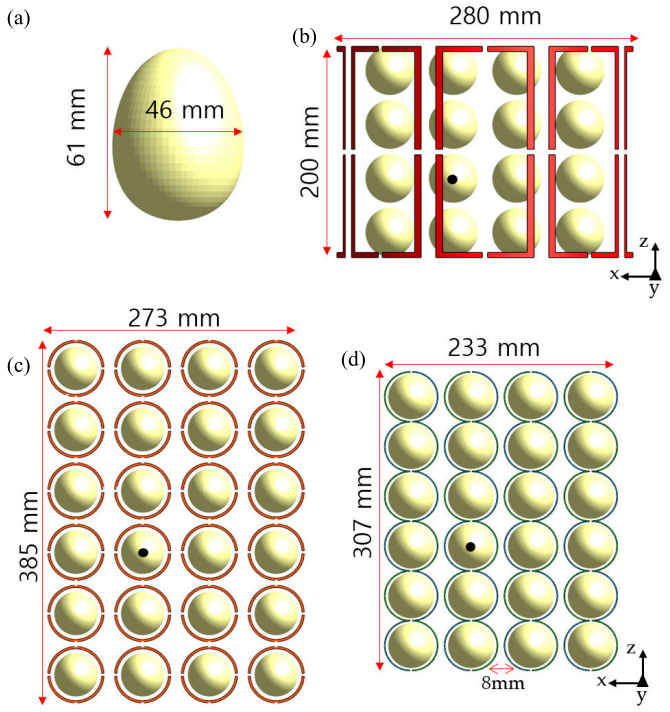

Fig. 2. Geometry of the: (a) egg model; (b) eight-channel loop array and 16 eggs; (c) 24 single-loop coils with 24 eggs; and (d) four braided multiple-turn coils with 24 eggs, displayed in the xz plane view.

In addition, the use of multiple turns increases the number of resonance modes. Therefore, for each turn, a resonance mode is generated. In this case, the choice of resonance mode at the right frequency is important. The admittance can be expressed as

$$Y = \left(\frac{1}{2\pi f L} + 2\pi f C\right)^n \tag{5}$$

where f denotes the frequency. The resonance frequency of the system occurs when Y is equal to zero. Multiple solutions can be identified due to the power n in the equation.

For a coil with n number of turns and identical value of capacitors, there is at least one resonance mode such that the produced $|B_1|$-field is uniform and identical for each turn, whereas the other resonance frequencies generate $|B_1|$-field only at some turns.

The proposed design is based on the model shown in Fig. 1(a) with a coil radius of 25 mm and a total length of 307 mm to accommodate six eggs. The space between the upper and lower layers is set to 1 mm, as shown in Fig. 1(b), and the location of tuning capacitors is indicated for each turn, while the end-tuning capacitor position and connection are shown in Fig. 1(c). The capacitors at the extremes are used to connect the upper and lower layers to complete the circuit. Similarly, the source indicated by the orange arrow is connected at the center of the coil in the upper layer. The model of the egg, as depicted in Fig. 2(a), possesses a height of 61 mm and a diameter of 46 mm.

We have compared the performance of the proposed coil with an eight-channel loop array coil, which has a cylindrical shape with a radius of 140 mm and length of 200 mm, as shown in Fig. 2(b). The dimensions of this coil are based on those used for human brain scans at 7T MRI. We have also compared the proposed coil with multiple single-channel loop coils with individual reception channels. Each loop coil has a radius of 27.5 mm and a separation of 5 mm in the z-axis, as shown in Fig. 2(c). To demonstrate the advantages of the proposed coil design, comprehensive simulations were conducted using different coil types in combination with multiple eggs. Specifically, for the eight-channel array coil, a total of 16 eggs were utilized, as this particular coil configuration was capable of accommodating only this quantity of eggs in the central plane. In contrast, both the single-loop coils and the proposed coil were evaluated using 24 eggs during the simulations. In the case of the proposed coil, four braided coils were employed, with each braided coil accommodating six eggs. The spacing between adjacent coils in the x-axis was set at 6 mm. A visual representation of the coil and egg models, as well as their arrangement, can be observed in Fig. 2(b)–(d).

B. EM Simulations

Based on the geometry and 3-D models, EM simulations were performed for each coil using the commercial finite-difference time-domain solver Sim4life (Zurich, ZTM). Each coil was tuned and matched to the operating frequency of a 7T MRI scanner corresponding to 297.4 MHz. The input voltage source was a Gaussian pulse with a central frequency of 297.4 MHz and a bandwidth of 600 MHz. All conductor lines were set as perfect electrical conductors (PECs). Fig. 2(a) depicts the egg model, characterized by a solid structure with uniform electrical properties. The conductivity and permittivity values assigned to the egg model are 2.2 S/m and 72.7, respectively, representing the electrical properties of cerebrospinal fluid (CSF) at a frequency of 297.4 MHz. Fig. 2(b)–(d) illustrates the configuration of the eight-channel array loop coils, the individual loop coils, and the proposed coil model, each indicating the placement of the eggs within the respective coil setups.

$|B_1|$-field maps were acquired for each egg using EM simulations and analyzed using statistical measurements, such as mean and coefficient of variation (CV), which is the standard deviation scaled by the mean value. The computed $|B_1|$-field for each coil was normalized to achieve 2 μT at the center of the coil configuration, which is shown by the black marker in Fig. 2(b)–(d), respectively.

C. Benchwork

The proposed coil was constructed based on the specified geometry, and to evaluate its versatility, a six-egg coil was fabricated. Printed circular copper lines were employed to create semicircles with a 25-mm radius, and the conductor lines had a width of 5 mm. The coils were positioned on an acrylic surface featuring a 25-mm-diameter hole to accommodate the eggs. The separation between the upper and lower layers was achieved using a 3-mm-thick acrylic sheet. Capacitors were carefully selected to enable tuning of the coil at the desired frequency. A T-network circuit configuration was

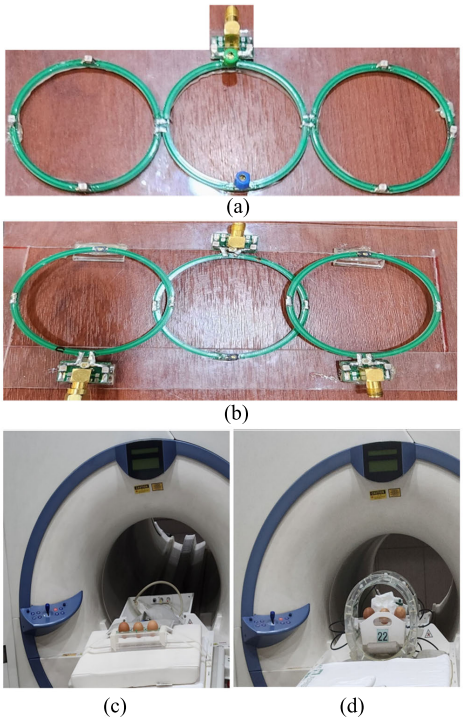

Fig. 3. Photograph of the developed: (a) braided coil and (b) single-loop coils, for three eggs. The integration with the MRI scanner of the: (c) braided coil and (d) head eight-channel array coil.

utilized for 50-Ω matching. Furthermore, reference loop coils were developed using the same conductor materials with a radius of 30 mm. Each coil was tuned to operate at 297.4 MHz and matched to 50 Ω. Decoupling between the reference loop coils was achieved by overlapping the distance between them.

In this study, a reference eight-channel array coil designed for TRx in head imaging was also incorporated. The coil's volume was defined by a 140 mm radius and a 200 mm length, and each individual coil within the array measured 200 mm in length and 90 mm in width. To facilitate TRx, all the coils were connected to a detuning circuit. A photograph of the proposed braid-shaped coil for three eggs is shown in Fig. 3(a), and the reference three-channel single-loop coils are shown in Fig. 3(b).

D. Magnetic Resonance Imaging

Images of each of the described coils were acquired with a 7T MRI scanner (Siemens, Erlangen, Germany, Magnetom) using a turbo spin echo pulse sequence. The pulse sequence had a repetition time (TR)/echo time (TE) of 6000 and 93 ms, respectively, and a flip angle of 90°. The matrix size was 352 × 512 × 18 with a field of view of 200× 140 × 36 mm. Images were acquired in the axial view (*xy* plane), with an average of 1. The dimensions of the scanner are 900-mm bore, with a diameter spherical volume (DSV) of 45 cm, which is a typical B_0-field homogeneity specification [14], with a gradient coil strength of 40 mT/m, in the *x*-, *y*-, and *z*-axes.

The eggs selected for imaging were nonfertilized chicken eggs suitable for consumption and purchased from a local store. Given that no living cells or objects were used in the experiment, consent from the Institutional Review Board was not required. The integration of the proposed coil and the head eight-channel coil with the scanner is shown in Fig. 3(c) and (d).

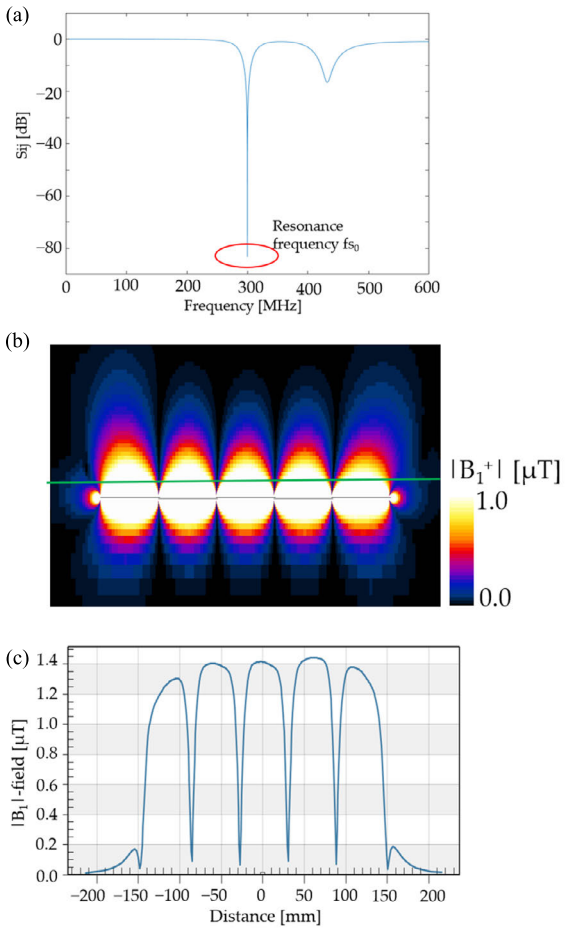

Fig. 4. (a) S11 parameters for the proposed coil showing the resonance frequency. (b) Computed $|B_1|$-field for the proposed coil (green line shows the place where the line profile is taken). (c) Line profile showing uniform field among each turn.

III. Results

The proposed design for multiple eggs based on braid-shaped radio frequency (RF) coil was tested with EM simulations, benchwork, and MR images, and the results obtained are presented as follows.

A. Simulations

EM simulations were first performed with the proposed coil in an empty space. The proposed coil was tuned with capacitors with the same value of 3.45 μF. Fig. 4(a) shows the S11 of the proposed coil, while Fig. 4(b) shows the computed $|B_1|$-field in the empty space in the *zy* plane. It can be observed that the $|B_1|$-field is uniform for each turn, and it has the same distribution. A line profile of the field along the *z*-axis for a distance of 5 mm [indicated by the green line in Fig. 4(b)] along the *y*-axis is plotted in Fig. 4(c), which shows that the field intensity has the same shape for each turn. This

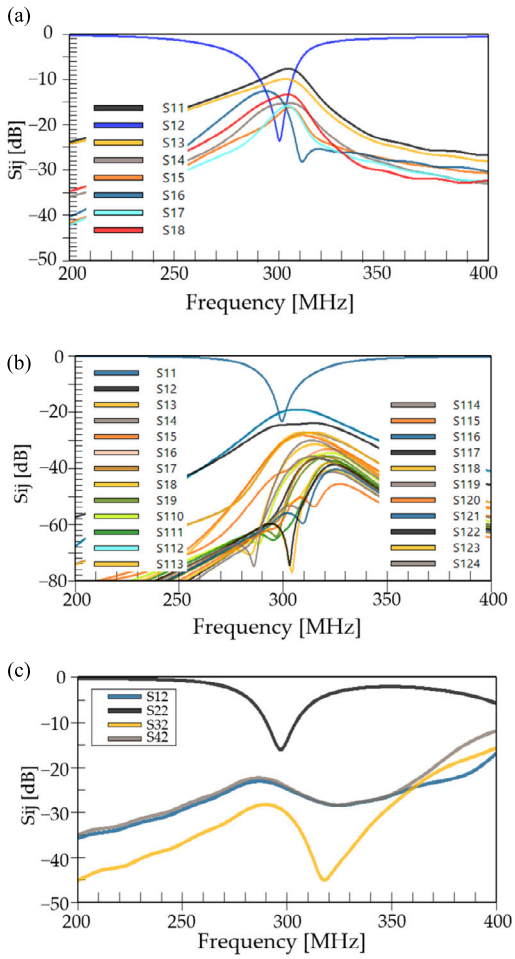

Fig. 5. Coupling analysis showing the Sij parameters for: (a) eight-channel array coil; (b) 24 single individual loop coils; and (c) proposed four braided coils.

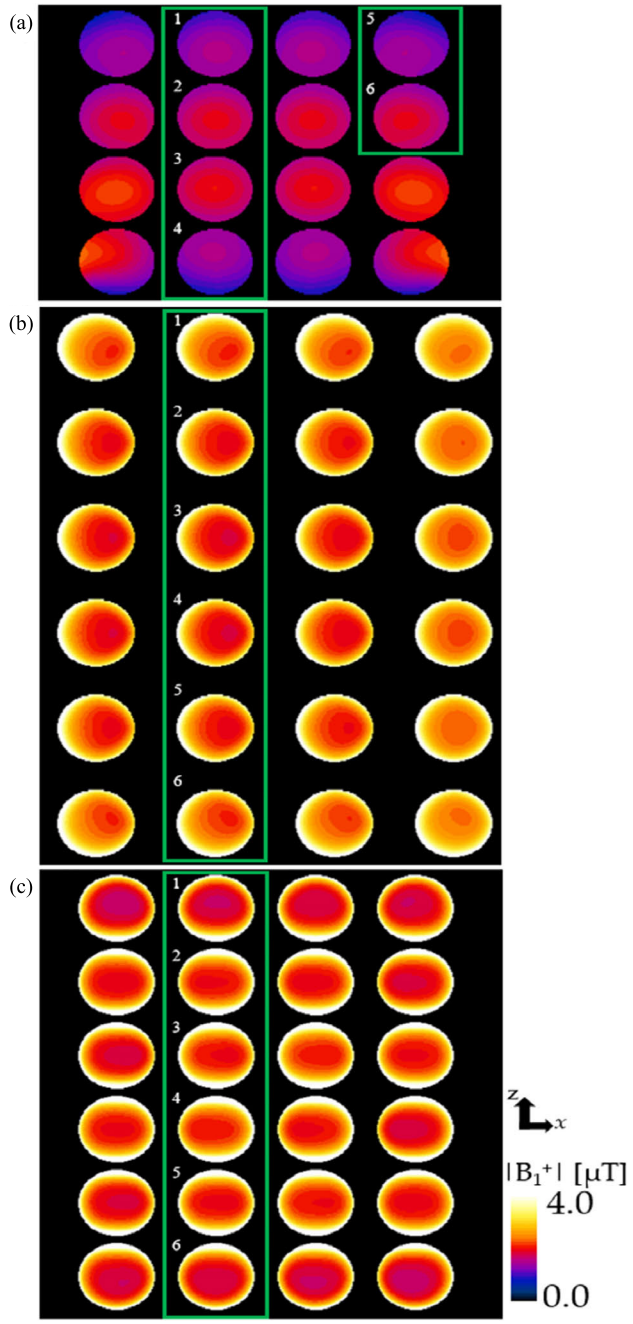

Fig. 6. Computed $|B_1|$-field for: (a) eight-channel array coil with 16 eggs; (b) single-loop coils with 24 eggs; and (c) proposed braid-shaped coil with 24 eggs. Displayed in the *xz* plane.

is of special interest as the egg models will be placed in that area. However, this model cannot be used for human imaging because the void regions between each turn of the coil reduce the field penetration and uniformity. An advantage of the proposed coil is that the imaging object is placed inside the coil.

Simulations were conducted using the egg models to compare the performance of the proposed coil with that of the single-loop coils and the volume eight-channel loop coil array. The coupling analysis, based on the Sij parameters, was performed, and the results are presented in Fig. 5(a)–(c), representing the eight-channel array, 24 single-loop coils, and the four braided coils, respectively. In the case of the eight-channel loop coil array, the coupling analysis reveals a maximum coupling of −8 dB. Comparatively, the single-loop coils exhibit a coupling of −14 dB, indicating a higher degree of coupling and complexity. However, the S-parameter plot for the braided coil demonstrates a better decoupling performance, with a coupling of −25 dB with adjacent coils and −32 dB with the farthest coil. These results highlight the superior decoupling capabilities of the braided coil design, offering significantly reduced coupling compared to the other coil configurations. These results indicate that the braided coil requires less decoupling requirements than the other types of coil, and in this way, the complexity of coil design can be reduced. The lower coupling requirement indicates that the proposed coil can be scaled to a larger number of elements.

In terms of performance that can translate to image capabilities, the $|B_1|$-field was also computed for each coil type. Fig. 6(a) shows the $|B_1|$-field of the 16 eggs for the eight-channel array coil, and Fig. 6(b) shows the field for the individual loop coils and 24 eggs, while the field for the proposed coil is shown in Fig. 6(c), with the 24 eggs. The $|B_1|$ fields are displayed on the *zx* plane, and it should be noticed the distribution and position of the eggs for each coil type,

TABLE I

SUMMARY OF $|B_1|$-FIELD FOR EACH EGG AND COIL IN TERMS OF (MEAN/CV)

Egg number	8-channel array	Single coils	Braided coil
Egg #1	1.31/0.11	1.75/0.62	1.78/0.48
Egg #2	1.66/0.08	1.62/0.64	1.82/0.46
Egg #3	1.72/0.07	1.55/0.65	1.80/0.47
Egg #4	1.29/0.12	1.55/0.67	1.85/0.46
Egg #5	1.25/0.14	1.62/0.65	1.77/0.47
Egg #6	1.64/0.11	1.76/0.64	1.70/0.48

TABLE II

SNR FOR EACH EGG USING EACH OF THE IMAGING COILS

Egg number	8-channel array	Single coils	Braided coil
Egg #1	115	168	300
Egg #2	96	177	288
Egg #3	164	67	297

which shows that the proposed coil can provide a uniform |B1|-field of similar intensity to the single-loop coils but it can reduce the space between eggs and therefore has a better efficiency in terms of filling factor. While the eight-channel coil can have the eggs in similar separation, the $|B_1|$-field is different between eggs. The mean value and CV for the eggs inside of the green box in Fig. 6 corresponding to each coil setup are summarized in Table I, where the first number corresponds to the mean value and the second number corresponds to the CV. The overall $|B_1|$-field means for the total eggs in the eight-channel, single-loop coil, and proposed coil are 1.5, 1.7, and 1.8 μT, respectively. It can be noticed for the case of the eight-channel array coil that the field intensity is larger at the center and lower at the sides. The single-loop coils provide a similar field intensity for each egg, but as mentioned before, the number of egg screens depends on the number of reception channels, and the position of the eggs is more sparser than the other coil setups. The field intensity of the braided coil produces a comparable field intensity to the loop coil, while only requiring using four channels to cover 24 eggs.

B. Benchwork

The proposed coil was built based on the simulated coils, as shown in Fig. 3. The coil is tuned and matched to 297 MHz and 50 Ω. To obtain the resonance frequency, we have adjusted the value of the capacitors in each turn. Fig. 7 shows the acquired S11 value for the proposed coil, and the 50-Ω matching condition was also obtained.

C. MR Images

MR images of three eggs were acquired using the constructed coils. Gradient echo images acquired are displayed in Fig. 8 for the eight-channel array, single coils, and proposed coil, respectively. The images acquired with the proposed coil were of higher quality than the other coils. A summary of the

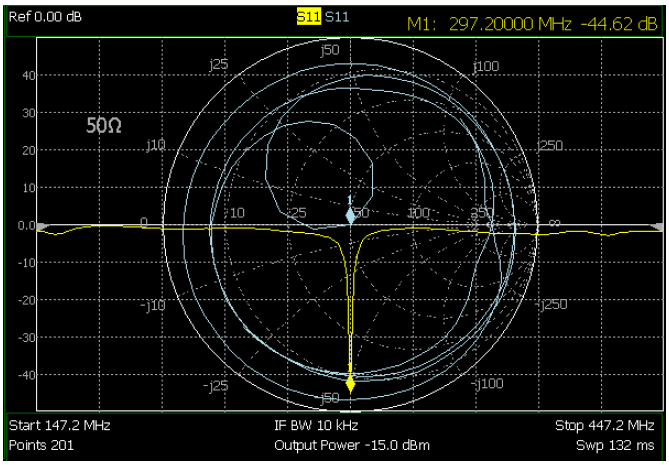

Fig. 7. Measured S11 parameter for the proposed coil showing the resonance mode and 50-Ω matching of the coil.

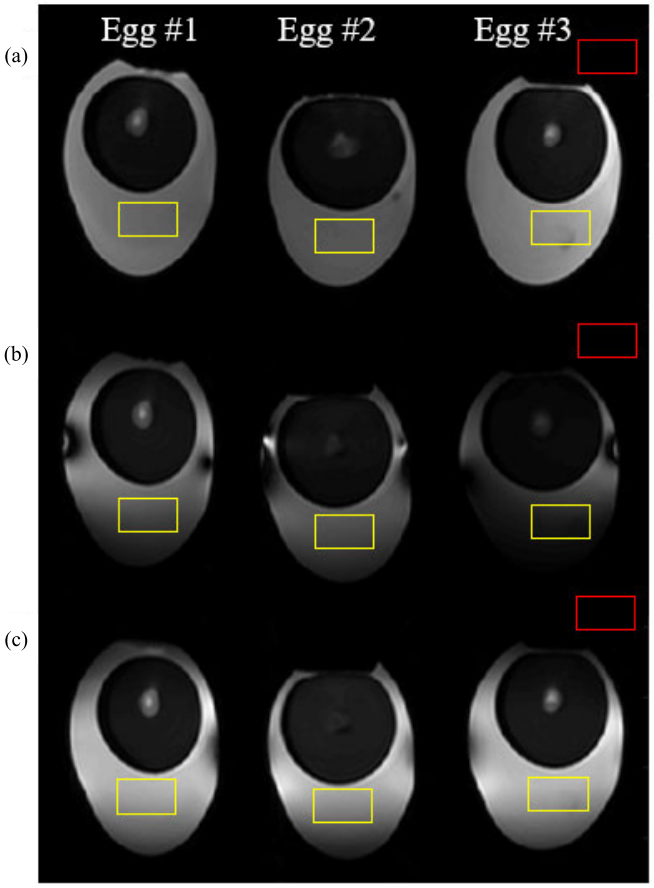

Fig. 8. Acquired turbo spin echo images for the: (a) eight-channel array coil; (b) single-loop coils; and (c) proposed multiturn coil. Showing the ROIs for statistical analysis.

statistical analyses for each egg is presented in Table II, for the region of interest (ROI) shown in Fig. 8 in a yellow box for each egg, and the background ROI is marked with a red box. The overall signal-to-noise ratios (SNRs) for the eight-channel-array, single coils, and proposed coil were 125, 137, and 296, respectively. The uniformity of the image was also computed with standard deviation between the ROI of each

egg, which was recorded as 35, 61, and 7 for the eight-channel array, single coils, and proposed coil, respectively. It can be noticed that the image acquired with the eight-channel array coil has a different image scale and the SNR on each coil depends on their position inside the coil. For the case of the image in Fig. 8(a), the lower image intensity is located at the center of the coil, and the higher intensity to the sides. The use of three single-loop coils has a higher SNR than the eight-channel array coil but less than the proposed coil; however, as mentioned before, it has a limitation on the number of receive and transmit channels. The use of single-loop coils shows artifacts near the area of the conductor line. The braided coil exhibits higher SNR and image quality across the eggs, while only requiring one receive and transmit channel. However, in a similar way to simulations, there is a higher image intensity near the coil conductor line.

The filling factor (*ff*) represents the ratio of the total volume occupied by the eggs *Ve* to the volume covered by the coil *Vc*

$$ff = Ve/Vc \tag{6}$$

a value close to unity indicates better space efficiency [15]. Each egg has a volume of 68 362 mm^3. In the case of the eight-channel array coil, it covered a volume of 226 × 63 × 200 mm, allowing for the imaging of only eight eggs while maintaining acceptable field intensity and uniformity. This resulted in a filling factor of 0.19. Alternatively, using single coils for 24 eggs required a larger volume of 260 × 63 × 371 mm to mitigate coupling between the coils. Despite the larger volume, the filling factor for the single coils was 0.27. In our proposed coil arrangement, consisting of four braided coils, we were able to cover 24 eggs within a volume of 226 × 63 × 302 mm, resulting in a filling factor of 0.38. This demonstrates improved space efficiency compared to the single-coil arrangement.

IV. Discussion

In this study, we proposed a novel concept for an RF coil that can be used for multiple egg imaging in MRI. The coil was designed in the shape of a braid with multiple turns. Individual eggs were placed in the central area. We performed EM simulations on the proposed coil to verify that the main resonance frequency is capable of producing a uniform $|B_1|$-field at each of the spaces between braided conductors. In particular, the concept could be extended to multiple turns while still providing a uniform field. A comparison of the $|B_1|$-field with the eight-channel array coil volume and single-loop coils demonstrated the advantage of the proposed coil, that is, it has an efficient field intensity and uniformity across the eggs, while reducing the TRx channels required.

The $|B_1|$-field intensity for each of the 24 eggs in the simulation had a CV of 0.4 by using the proposed coil, whereas the eight-channel array coil and single coils had a standard deviation of 0.5 and 0.7, respectively. This indicates that the proposed coil can provide similar field intensity to each egg, comparable to the single-loop coil case.

By optimizing the coil design and arrangement, we have achieved a higher filling factor, indicating better space utilization for imaging a larger number of eggs. This shows an improvement of two times compared with the eight-channel array coil and 1.42 times better than using single-loop coils. The proposed coil arrangement presents a promising solution for enhancing the efficiency and throughput of industrial processes related to egg imaging.

The proposed coil has the potential to significantly benefit the poultry industry by enabling the simultaneous acquisition of images from multiple eggs, thus achieving high throughput in the scanning process.

Therefore, the advantage of the proposed coil consists of providing a uniform field for each egg as in the case of single-loop coils, while allowing the placement of eggs in a tighter space similar to the eight-channel coil.

In this study, we also considered the construction of the proposed coil, in which the S11-parameter exhibited a pattern similar to that obtained with simulation.

The construction of the coil is not complicated; however, it should be noted that the tuning process could be complicated, as the values of capacitors should be carefully adjusted. In general, we have seen that the location of the main resonance frequency is usually the first and lower frequencies. During the benchwork development of the coil, a pick-up coil was used to verify that the amplitude of the induced current was similar at each turn.

One limitation of the proposed coil type is that it neglects the use of parallel imaging during reception. The objects lie in the interior of the turn and shared information is not available for the nearby coils to proceed with parallel reconstruction. However, the same argument is applicable for single-loop coils, when the imaging object is inside the loop coil because they are not capable of sharing spatial–temporal information sufficient for parallel reconstruction. Therefore, the eight-channel volume coil would be suitable; however, it has the limitation of poor image quality when compared with the proposed coil. Moreover, given the field patterns produced by the proposed coil structure has the potential to be used for simultaneous multislice (SMS) imaging [16]. SMS is an acquisition method where information of multiple slices is simultaneously encoded in the acquired data, and by using reconstruction algorithms, an individual image can be obtained with a reduced scan time. The proposed coil would suit well for this technique since the coil has good in-plane localization as well as a large coverture for multiple slices.

Although we have proposed the use of eggs as the imaging object, the proposed coil can also be used for any type of object that can be fit, such as cultured cells, phantoms, and even small animals.

Since the proposed coil is based on the loop geometry, it can work similarly at different frequencies. It should be expected that at lower frequencies the field would be more uniform than at higher frequencies.

In the future, we plan to perform biological and anatomical analyses of eggs using the proposed coil based on the growth of fertilized and unfertilized eggs.

V. Conclusion

In this study, we presented a coil that can acquire MR images of multiple eggs with a minimum number of TRx chan-

nels in addition to providing a high intensity and uniformity image quality for each egg. Hopefully, the proposed coil will be useful for further applications and studies of in-ovo MRI.

ACKNOWLEDGMENT

The authors are thankful to Minyeong Seo for providing coil simulation modeling.

REFERENCES

[1] A. G. Van der Kolk, J. Hendrikse, J. J. Zwanenburg, F. Visser, and P. R. Luijten, "Clinical applications of 7T MRI in the brain," *Eur. J. Radiol.*, vol. 82, no. 5, pp. 708–718, 2013.

[2] J. H. G. Helthuis et al., "High resolution 7T and 9.4T-MRI of human cerebral arterial casts enables accurate estimations of the cerebrovascular morphometry," *Sci. Rep.*, vol. 8, no. 1, pp. 1–8, Sep. 2018.

[3] B. P. Thomas et al., "High-resolution 7T MRI of the human hippocampus in vivo," *J. Magn. Reson. Imag., Off. J. Int. Soc. Magn. Reson. Med.*, vol. 28, no. 5, pp. 1266–1272, Nov. 2008.

[4] R. Klose et al., "Ultra-high-field MRI in the chicken embryo in ovo—A model for experimental ophthalmology," *Klinische Monatsblatter Augenheilkunde*, vol. 234, no. 12, pp. 1458–1462, 2017.

[5] B. Shojaei, H. Tavakoli, M. J. Aghasizade, and H. R. S. Badkhor, "Morphologic evaluation of the fertilized and unfertilized ostrich egg during the early stages of development (MRI analysis)," *Anatomical Sci. J.*, vol. 11, no. 4, pp. 169–174, 2014.

[6] T. Winkens et al., "In-ovo imaging using ostrich eggs—Evaluation of physiological embryonal development on computed tomography," *Acta Zoologica*, vol. 103, no. 4, pp. 492–502, Oct. 2022.

[7] B. De Ketelaere, P. Coucke, and J. De Baerdemaeker, "Eggshell crack detection based on acoustic resonance frequency analysis," *J. Agricult. Eng. Res.*, vol. 76, no. 2, pp. 157–163, Jun. 2000.

[8] S. W. Falen, N. M. Szeverenyi, D. S. Packard, and M. J. Ruocco, "Magnetic resonance imaging study of the structure of the yolk in the developing avian egg," *J. Morphol.*, vol. 209, no. 3, pp. 331–342, Sep. 1991.

[9] M. Johnson. (Nov. 2021). *MRI Technology Can Help Identify Which Eggs are Fertile*. [Online]. Available: https://www.wattagnet.com/latest-news/article/15534623/mri-technology-can-help-identify-which-eggs-are-fertile

[10] B. Gruber, M. Froeling, T. Leiner, and D. W. J. Klomp, "RF coils: A practical guide for nonphysicists," *J. Magn. Reson. Imag.*, vol. 48, no. 3, pp. 590–604, Sep. 2018.

[11] M. S. Ramirez, E. Esparza-Coss, and J. A. Bankson, "Multiple-mouse MRI with multiple arrays of receive coils," *Magn. Reson. Med.*, vol. 63, no. 3, pp. 803–810, Mar. 2010.

[12] S. E. Solis, R. Wang, D. Tomasi, and A. O. Rodriguez, "A multi-slot surface coil for MRI of dual-rat imaging at 4 T," *Phys. Med. Biol.*, vol. 56, no. 12, pp. 3551–3561, Jun. 2011.

[13] T. Nam et al., "Design of rotated surface coil array for multiple-subject imaging at 400 MHz," *IEEE Access*, vol. 10, pp. 66281–66289, 2022.

[14] H. M. Gach, A. N. Curcuru, S. Mutic, and T. Kim, "B0 field homogeneity recommendations, specifications, and measurement units for MRI in radiation therapy," *Med. Phys.*, vol. 47, no. 9, pp. 4101–4114, Sep. 2020.

[15] D. Papoti et al., "Segmented solenoid RF coils for MRI of ex vivo brain samples at ultra-high field preclinical and clinical scanners," *J. Magn. Reson. Open*, vols. 16–17, Dec. 2023, Art. no. 100103.

[16] M. Barth, F. Breuer, P. J. Koopmans, D. G. Norris, and B. A. Poser, "Simultaneous multislice (SMS) imaging techniques," *Magn. Reson. Med.*, vol. 75, no. 1, pp. 63–81, Jan. 2016.

Daniel Hernandez received the Ph.D. degree from Kyung Hee Universrity, Seoul, South Korea, in 2016.

He is currently working as a Research and Assistant Professor with the Department of Biomedical Engineering, Gachon University, Incheon, South Korea. His research interests are electromagnetic theory, simulations and development of antennas, and image and signal processing for magnetic resonance imaging (MRI) engineering.

Yonghwa Jeong received the M.S. degree from the Department of Health Sciences and Technology, Gachon University, Incheon, South Korea, in 2023.

His research interests include RF coil and electromagnetic simulation.

Kyoung-Nam Kim received the Ph.D. degree in electrical engineering and information technology from the University of Duisburg-Essen, Essen, Germany, in 2011.

He has been an Associate Professor with the Department of Biomedical Engineering, Gachon University, Seongnam, South Korea, since 2016. His research interests include medical electronic engineering, magnetic resonance imaging (MRI) systems, electromagnetic field analysis, and RF MRI coils.

Dr. Kim is currently an MRI Committee Member of the Korean Society of Magnetic Resonance in Medicine.